NIH Public Access
Author Manuscript
Atherosclerosis. Author manuscript; available in PMC 2012 December 1.

Published in final edited form as:
Atherosclerosis. 2011 December ; 219(2): 588–595. doi:10.1016/j.atherosclerosis.2011.07.128.

Vulnerable Plaque Features on Coronary CT Angiography as Markers of Inducible Regional Myocardial Hypoperfusion from Severe Coronary Artery Stenoses

Haim Shmilovich, MD[a,*], **Victor Y Cheng, MD**[a,b,*], **Balaji K Tamarappoo, MD, PhD**[a], **Damini Dey, PhD**[a,b], **Ryo Nakazato, MD, PhD**[a], **Heidi Gransar, MSc**[a], **Louise EJ Thomson, MBChB, MRCP**[a,b], **Sean W Hayes, MD**[a,b], **John D Friedman, MD**[a,b], **Guido Germano, PhD**[a,b], **Piotr J Slomka, PhD**[a,b], and **Daniel S Berman, MD**[a,b]

[a]Cedars-Sinai Heart Institute and the Departments of Imaging and Medicine, Cedars-Sinai Medical Center, Los Angeles, California, USA

[b]Department of Medicine, David Geffen School of Medicine, University of California, Los Angeles, California, USA

Abstract

Objective—We explored whether the presence of 3 known features of plaque vulnerability on coronary CT angiography (CCTA) – low attenuation plaque content (LAP), positive remodeling (PR), and spotty calcification (SC) – identifies plaques associated with greater inducible myocardial hypoperfusion measured by myocardial perfusion imaging (MPI).

Methods—We analyzed 49 patients free of cardiac disease who underwent CCTA and MPI within a 6-month period and were found on CCTA to have focal 70–99% stenosis from predominantly non-calcified plaque in the proximal or mid segment of 1 major coronary artery. Presence of LAP (≤30 Hounsfield Units), PR (outer wall diameter exceeds proximal reference by ≥5%), and SC (≤3mm long and occupies ≤90° of cross-sectional artery circumference) were determined. On MPI, reversible hypoperfusion in the myocardial territory corresponding to the diseased artery was quantified both as percentage of total myocardium ($RevTPD_{ART}$) by an automatic algorithm and as summed difference score (SDS_{ART}) by two experienced readers. $RevTPD_{ART}$≥3% and SDS_{ART}≥3 defined significant inducible hypoperfusion in the territory of the diseased artery.

Results—Plaques in patients with $RevTPD_{ART}$≥3% more frequently exhibited LAP (70% vs. 14%, p<0.001) and PR (70% vs. 24%, p=0.001) but not SC (55% vs. 34%, p=0.154). $RevTPD_{ART}$ increased from 1.3±1.2% in arteries with LAP−/PR− plaques to 3.2±4.3% with LAP+/PR− or LAP−/PR+ plaques to 8.3±2.4% with LAP+/PR+ plaques (p<0.001); SDS_{ART} showed a similar increase: 0.3±0.7 to 2.3±2.8 to 6.0±3.8 (p<0.001). Using the same LAP/PR categorization, there was a marked increase in the frequency of significant hypoperfusion as determined by both

© 2011 Elsevier Ireland Ltd. All rights reserved.

Corresponding Author: Victor Y. Cheng MD, 8700 Beverly Boulevard Taper Building Room 1258, Los Angeles, California 90048, United States, victor.cheng@cshs.org; Phone: 001-310-423-1666; Fax: 001-310-423-0811.
*Drs. Shmilovich and Cheng contributed equally

Disclosures: Drs. Berman, Germano, and Slomka receive QPS software royalties (Cedars-Sinai Medical Center, Los Angeles, California, USA).

Publisher's Disclaimer: This is a PDF file of an unedited manuscript that has been accepted for publication. As a service to our customers we are providing this early version of the manuscript. The manuscript will undergo copyediting, typesetting, and review of the resulting proof before it is published in its final citable form. Please note that during the production process errors may be discovered which could affect the content, and all legal disclaimers that apply to the journal pertain.

NIH-PA Author Manuscript
NIH-PA Author Manuscript
NIH-PA Author Manuscript

NIH-PA Author Manuscript

NIH-PA Author Manuscript

NIH-PA Author Manuscript

RevTPD$_{ART}$≥3% (1/19 to 10/21 to 9/9, p<0.001) and SDS$_{ART}$≥3 (1/19 to 8/21 to 8/9, p<0.001). LAP and PR, but not SC, were strong predictors of RevTPD$_{ART}$ and SDS$_{ART}$ in regression models adjusting for potential confounders.

Conclusions—Presence of low attenuation plaque and positive remodeling in severely stenotic plaques on CCTA is strongly predictive of myocardial hypoperfusion and may be useful in assessing the hemodynamic significance of such lesions.

Keywords

coronary artery stenosis; low attenuation plaque; positive remodeling; spotty calcification; myocardial perfusion

1. Introduction

Presence of severe coronary artery stenosis (≥70% diameter) is often used as a surrogate for myocardial blood flow compromise, based on hemodynamic studies demonstrating that severe coronary artery stenosis leads to stress-induced myocardial hypoperfusion [1,2]. Yet, a substantial proportion of severe coronary artery stenoses do not produce significant hypoperfusion on myocardial perfusion imaging (MPI) [3,4]. In the nuclear sub-study of the COURAGE (Clinical Outcomes Utilizing Revascularization and Aggressive Drug Evaluation) trial, 40% of patients with ≥70% diameter stenosis on invasive coronary angiography exhibited none or mild myocardial hypoperfusion on single-photon emission computed tomographic MPI (SPECT-MPI) [4].

Processes that can increase myocardial hypoperfusion, including arterial wall injury and endothelial dysfunction, have been associated with specific changes in coronary plaque appearance, such as development of intra-plaque lipid core and positive vessel remodeling [5]. Non-invasive detection of lipid core (appearing as “low-attenuation” plaque, LAP), outward or “positive” vessel remodeling (PR), and spotty calcification (SC) on coronary computed tomographic angiography (CCTA) has been linked to the risk of acute coronary syndrome, denoting these findings as markers of plaque vulnerability [6]. However, whether these 3 features have impact on myocardial perfusion has not been evaluated. We conducted an exploratory study to test the hypothesis that severe coronary artery stenoses caused by plaques exhibiting LAP, PR, and/or SC result in greater myocardial hypoperfusion than similar stenoses caused by plaques that do not exhibit these features.

2. Methods

2.1 Patient population

From April 2006 through March 2011, we identified 49 consecutive patients who met all of the following criteria: no prior myocardial infarction or coronary artery revascularization, underwent both CCTA and SPECT-MPI or positron-emission tomography (PET)-MPI within a 6-month period at our center, CCTA showed severe single-vessel coronary artery stenosis from a discrete, predominantly non-calcified atherosclerotic plaque (<50% calcified component by visual estimation of whole plaque volume) causing 70–99% diameter stenosis in the proximal or mid left anterior descending (LAD), left circumflex (LCX), or dominant right coronary arteries (RCA), and no contraindications (≥50% left main stenosis, coronary artery anomaly, suspected total occlusion on CCTA defined as contrast absence for ≥5mm of contiguous plaque length, visible collateral circulation on CCTA, or acute coronary event or coronary artery revascularization between CCTA and MPI). Stenosis severity was manually quantified by an experienced, blinded reader using the luminal diameter ratio between the sites of maximal stenosis and proximal healthy reference [7]. Two patients had

NIH-PA Author Manuscript

NIH-PA Author Manuscript

NIH-PA Author Manuscript

CCTA and MPI on the same day, 19 had MPI after CTA (median 14 days, range 0–142 days), and 28 had MPI before CTA (median 12 days, range 1–150 days). All patients signed an informed consent, and this study was approved by our local Institutional Review Board.

2.2 SPECT-MPI and PET-MPI performance

For SPECT, patients discontinued beta-blockers and calcium channel-antagonists 48 hours and nitrates 24 hours before testing. Rest perfusion images were acquired after infusion of 7–9mCi of ^{99m}technetium (Tc)-sestamibi or 3–4.5mCi of ^{201}thallium (Tl). Exercise testing was performed with a symptom-limited Bruce treadmill exercise protocol. At near-peak heart rate, ^{99m}Tc-sestamibi (32–40mCi) was injected intravenously, after which exercise continued at maximal workload for 1 minute. MPI began 15–30 minutes after ^{99m}Tc-sestamibi injection. For vasodilator stress testing, adenosine was infused at 140 μg/kg/min for 5 minutes, with injection of 32–40mCi of ^{99m}Tc-sestamibi 2 minutes into infusion and imaging performed as previously described [8]. Images were acquired on a 2-detector gamma camera (Philips Adac-Forte, Philips Medical Systems, Cleveland, Ohio, USA or E-Cam, Siemens Medical Solutions, Forchheim, Germany) with high-resolution collimators. Acquisition consisted of 64 projections over a 180° orbit, performed only in supine position at rest and both supine and prone positions after exercise or adenosine vasodilation [9].

PET-MPI was performed using intravenous rubidium-82 (^{82}Rb). Patient preparation was same as that for SPECT. All images were acquired on a contemporary PET/CT scanner (Biograph-64, Siemens Medical Solutions, Forchheim, Germany). At rest, in supine position, 25–40mCi of ^{82}Rb was infused, and data acquisition in list-mode began at infusion initiation and continued for 7 minutes. Following rest acquisition, intravenous adenosine was infused at a rate of 140 μg/kg/min for 7 minutes. Two minutes into adenosine infusion, 25–40mCi of ^{82}Rb was administered, and data acquisition was performed for 7 minutes. In both states, non-contrast CT scans for attenuation correction was obtained using the following parameters: spiral-mode, 3mm slice thickness, 3.36 second scan time, 1.5 pitch, 0.5 second rotation time, 1.2×24mm collimation and 120kVp tube voltage. CT-based attenuation correction was used to generate reconstructed axial scintigraphic data. Short-axis, vertical long-axis, and horizontal long-axis tomograms were generated from data collected 2–6 minutes after ^{82}Rb infusion.

2.3 MPI analysis

All MPI studies were prospectively analyzed using an automated computer algorithm (QPS for SPECT, QPET for PET, Los Angeles, California, USA) [10]. Automatically-generated myocardial contours from this algorithm were checked and, if necessary, adjusted to best fit the myocardium by a blinded experienced reader. Default myocardial segmentation and vessel assignment were based on the 17-segment American Heart Association model [11]. When appropriate, vessel assignments were adjusted using input from a CCTA reader. To quantify myocardial perfusion, we used the validated, automated measure of total perfusion deficit (TPD) and reader-determined summed difference score (SDS). TPD combines extent and severity of myocardial signal attenuation and expresses detected hypoperfusion as a percentage of total myocardium [10,12]. Supine TPD was automatically computed at rest and during stress using established normal limits for ^{99m}Tc [10] and ^{82}Rb [13]. Difference in TPD between stress and rest defined “reversible TPD” (RevTPD). SDS was defined as the difference in total segmental radionuclide uptake score between stress and resting images (each of the 17 myocardial segments were scored from 0 to 4 in both states; 0 = normal, 1 = equivocal, 2 = moderately reduced, 3 = severely reduced, 4 = no uptake) and was obtained by consensus from 2 experienced, blinded readers [14]. RevTPD and SDS were each further divided into 3 component values according to the distributions of the LAD, LCX, and RCA. Only RevTPD and SDS corresponding to the artery of interest ($RevTPD_{ART}$ and SDS_{ART})

NIH-PA Author Manuscript

NIH-PA Author Manuscript

NIH-PA Author Manuscript

were analyzed. $RevTPD_{ART}$≥1% was considered detectable. For $RevTPD_{ART}$, ≥3% was criterion for significant hypoperfusion [9]. For SDS_{ART}, ≥3 was criterion for significant hypoperfusion.

2.4 CCTA performance

CCTA was performed on a dual-source CT scanner (SOMATOM Definition, Siemens Medical Solutions). Beta-blockade with metoprolol was used to achieve a heart-rate of <70 beats-per-minute, and 0.4mg nitroglycerin spray (Sciele Pharma, Alpharetta, Georgia, USA) was administered 3–5 minutes prior to the scan. Eighty ml of intravenous contrast (Omnipaque, General Electric Healthcare, Princeton, New Jersey, USA) followed by 50–80ml of saline at a rate of 5ml/s were power-injected into the antecubital vein. Ascending aorta contrast-triggered (100 Hounsfield Units), ECG-gated scanning was then performed in one breath-hold. Scanning parameters included heart-rate dependent pitch (0.2–0.45), 330ms gantry rotation-time, 100 or 120kVp tube-voltage depending on patient body-mass index [15], and 330–350mAs reference tube current. Acquired CCTA data was reconstructed in mid-diastole and at end-systole using 0.6mm slice-thickness (0.75mm if BMI was >35kg/m^2), 0.3mm slice increment, 250mm field-of-view, 512×512 matrix, and B26f "medium-smooth" kernel.

2.5 Plaque analysis on CCTA

Plaque assessment on CCTA was independently performed by 2 blinded experienced readers using axial images, oblique multiplanar reformations, and oblique maximum intensity projections [16]. Plaque length was measured using curved multiplanar projection (Sureplaque, Vital Images, Minnetonka, Minnesota, USA). For each plaque of interest, readers independently determined the presence of LAP, defined as visually distinct intra-plaque hypodensity containing Hounsfield Unit ≤30, SC, defined as discrete calcification ≤3mm in length and occupying ≤90° arc when viewed in vessel short-axis, and PR, defined as maximal outer arterial wall diameter along the plaque exceeding proximal reference by ≥5% (Figure 1). Each reader also examined the artery and branches distal to the plaque of interest for presence of ≥50% diameter stenosis. Results obtained by each reader were separately recorded to assess reproducibility. Consensus was used to resolve discrepancies.

2.6 Statistical methods

Continuous variables were described as median with inter-quartile range or mean with standard deviation. Categorical variables were described as frequencies. Variables with verified normal distributions were compared using the Student's t-test (for 2 groups) and one-way analysis-of-variance (for >2 groups); for non-normally distributed variables, the nonparametric Wilcoxon rank-sum test (for 2 groups) and Kruskal-Wallis test (for >2 groups) were used. Comparison of binary variables was performed using the chi-squared test or Fischer-Exact test, as appropriate. Linear regression analyses ($RevTPD_{ART}$ and SDS_{ART} as continuous outcomes) and logistic regression analyses ($RevTPD_{ART}$≥3% and SDS_{ART}>3 as binary outcomes) were performed to identify key predictors. First, the primary predictors of interest (presence of LAP, PR, and SC) were each assessed in pair-wise fashion with covariates that have been independently associated with myocardial hypoperfusion (sex, diabetes mellitus, smoking, stenosis severity, and downstream ≥50% diameter-stenosis) or have a plausible mechanism for affecting myocardial perfusion (coronary artery distribution, proximal plaque location, plaque length, and whether PET-MPI was performed). Regression was then repeated while simultaneously controlling for multiple aforementioned variables to examine robustness of pair-wise findings. To reduce the problem from over-fitting during multivariable regression, we limited covariates in the models to stenosis severity, coronary artery distribution, proximal plaque position, and parameters found to occur at a higher frequency in patients with $RevTPD_{ART}$≥3% with a comparison p-value <0.3 (diabetes,

NIH-PA Author Manuscript

NIH-PA Author Manuscript

NIH-PA Author Manuscript

smoking, and performance of PET-MPI, see Table 1). A p-value <0.05 was considered significant. Statistical analyses were performed using STATA software (version 10.0, College-Station, Texas, USA).

3. Results

O f the 49 patients studied, 34 were men (69%), and median age was 66 years. Ten patients had $RevTPD_{ART}$=0%, and 34 had $RevTPD_{ART}$≥1%, including 20 with $RevTPD_{ART}$≥3% (range 3.2–11.4%). Locations of the severely stenotic plaques in these 20 patients were: 10 proximal and 3 mid LAD, 1 proximal and 2 mid LCX, and 3 proximal and 1 mid RCA. Reference luminal diameter on CCTA ranged between 2–5.5mm with a median of 3.25mm. Comparisons of demographic and coronary artery plaque anatomic characteristics in patients with and without $RevTPD_{ART}$≥3% are shown in Table 1. Patients with $RevTPD_{ART}$≥3% had a higher rate of diabetes (60% vs. 14%, p=0.001) and were more likely to exhibit LAP (70% vs. 14%, p<0.001) and PR (70% vs. 24%, p=0.001), but not SC (55% vs. 34%, p=0.154). Based on the lack of difference in SC rates, patients were additionally compared between those exhibiting LAP (LAP+) or PR (PR+) (n=30, including 9 with LAP+/PR+) and those without either feature (LAP−/PR−, n=19) (Table 1). The sole demographic difference was a higher diabetes prevalence in patients with LAP+ and/or PR+ plaques (43% vs. 16%, p=0.045).

Unadjusted relationships between presence of LAP and PR and measures of inducible myocardial hypoperfusion are shown in Figure 2. $RevTPD_{ART}$ increased from 1.3±1.2% in patients with LAP−/PR− plaques to 3.2±3.2% in those with LAP+/PR- or LAP−/PR+ plaques to 8.3±2.4% in those with LAP+/PR+ plaques (p<0.001). A similar increase was seen with SDS_{ART} (0.3±0.7 to 2.3±2.8 to 6.0±3.8, p<0.001). Occurrence of $RevTPD_{ART}$≥3% and SDS_{ART}≥3 increased markedly from patients with LAP−/PR− plaques to those with LAP+/PR− or LAP−/PR+ plaques to those with LAP+/PR+ plaques ($RevTPD_{ART}$: 1/19 to 10/21 to 9/9, p<0.001; SDS_{ART}: 1/19 to 8/21 to 8/9, p<0.001). Within each of these 3 groups, comparison of patients with and without SC did not result in a significant difference in $RevTPD_{ART}$ or SDS_{ART}. In the 6 patients with ≥50% stenosis downstream from the principal plaque of interest, $RevTPD_{ART}$ was similar to the other 43 patients (2.1±2.8% vs. 3.5±3.5%, p=0.341). Examples of LAP and PR containing plaques and corresponding MPI results are shown in Figure 3.

In pair-wise regression analyses, presence of LAP and PR were strongly associated with $RevTPD_{ART}$ and $RevTPD_{ART}$≥3%, irrespective of the covariate. For $RevTPD_{ART}$, linear regression beta coefficients ranged from 3.08 to 3.82 for LAP (all p values ≤0.001) and from 3.17 to 3.75 for PR (all p values <0.001). For $RevTPD_{ART}$≥3%, odd sratios ranged from 2.9 to 4.3 for LAP (all p values <0.001) and from 1.8 to 2.3 for PR (p values ranged from 0.002 to 0.006). Pair-wise regression analyses using SDS_{ART} and SDS_{ART}≥3 yielded similar results. SC was not associated with $RevTPD_{ART}$, $RevTPD_{ART}$≥3%, SDS_{ART}, or SDS_{ART}≥3 in any pair-wise regression model. In multivariable regression analyses (Tables 2 and 3), presence of LAP and PR were robustly associated with $RevTPD_{ART}$ (p=0.004 for LAP and 0.001 for PR), SDS_{ART} (p=0.004 for LAP and 0.007 for PR), $RevTPD_{ART}$≥3% (OR=69.4, p=0.012 for LAP; OR=27.4, p=0.013 for PR), and SDS_{ART}≥3 (OR=15.3, p=0.023 for LAP; OR=27.4, p=0.036 for PR). SC showed no independent association with measures of myocardial hypoperfusion.

Consensus interpretation identified 18 with LAP, 21 with PR, and 21 plaques with SC. Inter-reader agreement was found in 42 cases for LAP (86%), 39 cases for PR (80%) and 44 cases for SC (90%).

NIH-PA Author Manuscript

NIH-PA Author Manuscript

NIH-PA Author Manuscript

4. Discussion

In this study we demonstrated a novel relationship between coronary artery plaque morphology and myocardial hypoperfusion. In severely stenotic plaques, noninvasive detection of LAP and PR – 2 vulnerable plaque features linked to risk of acute coronary syndrome – was highly associated with increased myocardial hypoperfusion by quantitative MPI. Severe stenoses from plaques without LAP and PR produced low amounts of myocardial hypoperfusion. Importantly, these strong relationships were found despite no measurable difference in stenosis severity and after adjusting for plaque location.

A handful of prior studies have evaluated the interaction between plaque composition and myocardial hypoperfusion. Lin et al. reported that presence of partially calcified plaque predicted ECG findings of inducible ischemia during exercise treadmill testing [17]. Bauer, et al. showed that non-calcified plaque volume on CCTA was associated with reversible myocardial hypoperfusion [18]. More recently, van Velzen et al. found that patients with ≥3 mixed plaques on CCTA were more likely to demonstrate reversible myocardial hypoperfusion on SPECT-MPI [19]. Our work is the first to extend these observations to the level of the individual coronary artery plaque. In doing so, we found that the presence of either LAP or PR identified virtually all plaques responsible for significant myocardial hypoperfusion. Importantly, LAP and PR are binary features with strict definitions that can be rapidly assessed, augmenting their appeal for clinical use.

Several potential explanations for the observed relationship between LAP, PR, and myocardial hypoperfusion should be considered. Severe stenoses containing either of these 2 features might have been present in coronary arteries that harbored greater endothelial dysfunction, supplied a larger extent of myocardium, had more extensive downstream atherosclerotic burden, were affected by microvascular disease, or possessed some combination of these factors. By limiting our evaluation to patients with focal severe stenosis in the proximal or mid-segment of a major coronary artery, we intended to reduce the variability in amount of affected myocardial territory and to lessen the impact of diffuse disease; nevertheless, contribution from these mechanisms could not be fully excluded. The possibility that LAP and PR may be markers of endothelial dysfunction should be considered. LAP has been correlated to the presence of a lipid or necrotic plaque-core [6,20,21], which forms from oxidative endothelial damage and is direct evidence of arterial wall injury [22,23]. LAP is intimately tied to concurrent presence of PR [24,25] and has been associated with reduction in local coronary artery blood flow attributed to endothelial dysfunction in intermediately-stenotic plaques [26].

Presence of SC did not predict increased myocardial hypoperfusion in our study. This finding parallels the work by Motoyama et al. that first demonstrated an independent relationship between SC and acute coronary syndrome, where SC had the lowest positive and negative predictive values (77% and 65%, respectively) when compared to LAP and PR [27]. Although yet to be proven, it is possible that SC occurs during both adverse remodeling and stabilization of coronary arterial plaque, negating its usefulness as a marker of increased arterial dysfunction.

The criteria we used to identify LAP, PR, and SC were based on definitions with prognostic importance in existing literature [27,28]. To identify LAP, we required visual recognition of low-attenuation and Hounsfield Unit verification. This was meant to emulate the everyday approach of current clinical cardiac imagers, who are not likely to measure Hounsfield Units in every non-calcified coronary artery plaque. Overall, we found the inter-observer reproducibility of these criteria to be promising in the hands of experienced readers.

NIH-PA Author Manuscript

NIH-PA Author Manuscript

NIH-PA Author Manuscript

In our study, absence of LAP and PR in the severely stenotic plaque accompanied a very low chance of significant myocardial hypoperfusion (5%), while concurrent presence of both features was uniformly associated significant myocardial hypoperfusion (9/9 had $RevTPD_{ART} \geq 3\%$, and 8/9 had $SDS_{ART} \geq 3$), suggesting that important hemodynamic significance information can be obtained with plaque characterization on CCTA. These findings may prove useful in managing stable patients with newly-diagnosed severe coronary artery disease. For example, a patient with severe stenosis from a plaque containing both LAP and PR may be considered at sufficiently high probability of significant inducible myocardial hypoperfusion, such that invasive angiography-based treatment approach after the CCTA would be preferred.

We recognize several limitations in the present work. This was a single-center study with a small sample size. Study patients were subject to referral bias; however, plaque-feature driven bias was unlikely, since descriptions of LAP, PR, and SC were not part of clinical CCTA reporting at the time these patients were imaged. We included patients who underwent SPECT-MPI or PET-MPI; adjustment for PET-MPI did not affect our findings. Sensitivity of LAP for true lipid core detection is known to be modest, and the criteria we employed (requiring both visual detection and Hounsfield Units verification) likely increased specificity and lowered sensitivity. However, our results suggest that the lipid cores missed by these criteria had a much weaker relationship to myocardial hypoperfusion. CT-based calculation of stenosis severity may have overestimated the degree of stenosis as measured on invasive coronary angiography; however, this should have affected all study plaques similarly rather than selectively biasing overestimation towards subgroups. Some patients may have had collateral circulation to the affected artery and/or significant small vessel disease not detected by CCTA due to limitations in spatial resolution. Future validation of our findings with invasive angiography-confirmed stenosis severity is thus needed. Plaques causing 50–70% diameter stenosis were not included, since less than 30% of these stenoses have been associated with significant ischemia on SPECT and PET-MPI [29,30]. Predominantly calcified plaques were not studied because calcium-related artifact from such plaques reduces the accuracy of stenosis quantification and renders detection of LAP and PR unreliable [31]. Application of our findings should be limited to severely-stenotic, predominantly non-calcified plaques on CCTA.

5. Conclusions

In this exploratory study, severe coronary arterial stenoses on CCTA from plaques exhibiting low-attenuation plaque and positive remodeling were strongly related to greater inducible myocardial hypoperfusion. These findings were independent of stenosis severity and indicate that plaque content and morphology may be useful in assessing the hemodynamic significance of severe stenoses.

Acknowledgments

Funding: Fellowship grant, American Physician-Fellowship for Medicine in Israel (Dr. Shmilovich); National Heart, Lung, and Blood Institute (Dr. Cheng, 1K23HL107458-01); American Heart Association Grant-in-Aid (Dr. Dey, 09GRNT2330000); The Lincy and Glazer Foundations (Beverly Hills, California, USA). Funding sources had no role in research conduct or preparation of the manuscript.

References

1. Ritchie J, Hamilton G, Gould K, Allen D, Kennedy J, Hammermeister K. Myocardial imaging with indium- 113m- and technetium-99m-macroaggregated albumin. New procedure for identification of stress-induced regional ischemia. Am J Cardiol. 1975; 35:380–9. [PubMed: 1090141]

NIH-PA Author Manuscript

NIH-PA Author Manuscript

NIH-PA Author Manuscript

2. Gould K, Lipscomb K, Hamilton G. Physiologic basis for assessing critical coronary stenosis. Instantaneous flow response and regional distribution during coronary hyperemia as measures of coronary flow reserve. Am J Cardiol. 1974; 33:87–94. [PubMed: 4808557]

3. Bateman T, Heller G, McGhie A, et al. Diagnostic accuracy of rest/stress ECG-gated Rb-82 myocardial perfusion PET: comparison with ECG-gated Tc-99m sestamibi SPECT. J Nucl Cardiol. 2006; 13:24–33. [PubMed: 16464714]

4. Shaw L, Berman D, Maron D, et al. Optimal medical therapy with or without percutaneous coronary intervention to reduce ischemic burden: results from the Clinical Outcomes Utilizing Revascularization and Aggressive Drug Evaluation (COURAGE) trial nuclear substudy. Circulation. 2008; 117:1283–91. [PubMed: 18268144]

5. Lavi S, Bae J, Rihal C, et al. Segmental coronary endothelial dysfunction in patients with minimal atherosclerosis is associated with necrotic core plaques. Heart. 2009; 95:1525–30. [PubMed: 19497916]

6. Pundziute G, Schuijf J, Jukema J, et al. Evaluation of plaque characteristics in acute coronary syndromes: non-invasive assessment with multi-slice computed tomography and invasive evaluation with intravascular ultrasound radiofrequency data analysis. Eur Heart J. 2008; 29:2373–81. [PubMed: 18682447]

7. Cheng V, Gutstein A, Wolak A, et al. Moving beyond binary grading of coronary arterial stenoses on coronary computed tomographic angiography: insights for the imager and referring clinician. JACC Cardiovasc Imaging. 2008; 1:460–71. [PubMed: 19356468]

8. Berman D, Kang X, Hayes S, et al. Adenosine myocardial perfusion single-photon emission computed tomography in women compared with men. Impact of diabetes mellitus on incremental prognostic value and effect on patient management. J Am Coll Cardiol. 2003; 41:1125–33. [PubMed: 12679212]

9. Nishina H, Slomka P, Abidov A, et al. Combined supine and prone quantitative myocardial perfusion SPECT: method development and clinical validation in patients with no known coronary artery disease. J Nucl Med. 2006; 47:51–8. [PubMed: 16391187]

10. Slomka P, Nishina H, Berman D, et al. Automated quantification of myocardial perfusion SPECT using simplified normal limits. J Nucl Cardiol. 2005; 12:66–77. [PubMed: 15682367]

11. Berman D, Abidov A, Kang X, et al. Prognostic validation of a 17-segment score derived from a 20-segment score for myocardial perfusion SPECT interpretation. J Nucl Cardiol. 2004; 11:414–23. [PubMed: 15295410]

12. Xu Y, Fish M, Gerlach J, et al. Combined quantitative analysis of attenuation corrected and non-corrected myocadial perfusion SPECT: Method development and clinical validation. J Nucl Cardiol. 2010

13. Piotr S, Sharmila D, Daniel B, James G, Guido G, Marcelo D. Automated quantification and normal limits for myocardial perfusion stress/rest Rb-82 PET/CT. SNM 2009 Annual Meeting. 2009

14. Hachamovitch R, Berman DS, Kiat H, et al. Exercise myocardial perfusion SPECT in patients without known coronary artery disease: incremental prognostic value and use in risk stratification. Circulation. 1996; 93:905–14. [PubMed: 8598081]

15. Gutstein A, Dey D, Cheng V, et al. Algorithm for radiation dose reduction with helical dual source coronary computed tomography angiography in clinical practice. J Cardiovasc Comput Tomogr. 2008; 2:311–22. [PubMed: 19083968]

16. Ferencik M, Ropers D, Abbara S, et al. Diagnostic accuracy of image postprocessing methods for the detection of coronary artery stenoses by using multidetector CT. Radiology. 2007; 243:696–702. [PubMed: 17517929]

17. Lin F, Shaw L, Berman D, et al. Multidetector computed tomography coronary artery plaque predictors of stress-induced myocardial ischemia by SPECT. Atherosclerosis. 2008; 197:700–9. [PubMed: 17720167]

18. Bauer R, Thilo C, Chiaramida S, Vogl T, Costello P, Schoepf U. Noncalcified atherosclerotic plaque burden at coronary CT angiography: a better predictor of ischemia at stress myocardial perfusion imaging than calcium score and stenosis severity. AJR Am J Roentgenol. 2009; 193:410–8. [PubMed: 19620437]

NIH-PA Author Manuscript

NIH-PA Author Manuscript

NIH-PA Author Manuscript

19. van Velzen J, Schuijf J, van Werkhoven J, et al. Predictive Value of Multislice Computed Tomography Variables of Atherosclerosis for Ischemia on Stress-Rest Single Photon Emission Computed Tomography (SPECT). Circ Cardiovasc Imaging. 2010
20. Brodoefel H, Burgstahler C, Heuschmid M, et al. Accuracy of dual-source CT in the characterisation of non-calcified plaque: use of a colour-coded analysis compared with virtual histology intravascular ultrasound. Br J Radiol. 2009; 82:805–12. [PubMed: 19332517]
21. Soeda T, Uemura S, Morikawa Y, et al. Diagnostic accuracy of dual-source computed tomography in the characterization of coronary atherosclerotic plaques: Comparison with intravascular optical coherence tomography. Int J Cardiol. 2009
22. Libby P. Inflammation in atherosclerosis. Nature. 2002; 420:868–74. [PubMed: 12490960]
23. Wentworth PJ, Nieva J, Takeuchi C, et al. Evidence for ozone formation in human atherosclerotic arteries. Science. 2003; 302:1053–6. [PubMed: 14605372]
24. Inaba S, Okayama H, Funada J, et al. Relationship between smaller calcifications and lipid-rich plaques on integrated backscatter-intravascular ultrasound. Int J Cardiol. 2010; 145:347–8. [PubMed: 20042247]
25. Schmid M, Pflederer T, Jang IK, et al. Relationship between degree of remodeling and CT attenuation of plaque in coronary atherosclerotic lesions: an in-vivo analysis by multi-detector computed tomography. Atherosclerosis. 2008; 197:457–64. [PubMed: 17727859]
26. Tanaka S, Noda T, Segawa T, et al. Relation between functional stenosis and tissue characterization of intermediate coronary plaques in patients with stable coronary heart disease. J Cardiol. 2010; 55:296–302. [PubMed: 20350522]
27. Motoyama S, Kondo T, Sarai M, et al. Multislice computed tomographic characteristics of coronary lesions in acute coronary syndromes. J Am Coll Cardiol. 2007; 50:319–26. [PubMed: 17659199]
28. Motoyama S, Sarai M, Harigaya H, et al. Computed tomographic angiography characteristics of atherosclerotic plaques subsequently resulting in acute coronary syndrome. J Am Coll Cardiol. 2009; 54:49–57. [PubMed: 19555840]
29. Di Carli MF, Dorbala S, Curillova Z, et al. Relationship between CT coronary angiography and stress perfusion imaging in patients with suspected ischemic heart disease assessed by integrated PET-CT imaging. J Nucl Cardiol. 2007; 14:799–809. [PubMed: 18022106]
30. Tamarappoo BK, Gutstein A, Cheng VY, et al. Assessment of the relationship between stenosis severity and distribution of coronary artery stenoses on multislice computed tomographic angiography and myocardial ischemia detected by single photon emission computed tomography. J Nucl Cardiol. 2010; 17:791–802. [PubMed: 20425027]
31. Brodoefel H, Burgstahler C, Tsiflikas I, et al. Dual-source CT: effect of heart rate, heart rate variability, and calcification on image quality and diagnostic accuracy. Radiology. 2008; 247:346–55. [PubMed: 18372455]

NIH-PA Author Manuscript

NIH-PA Author Manuscript

NIH-PA Author Manuscript

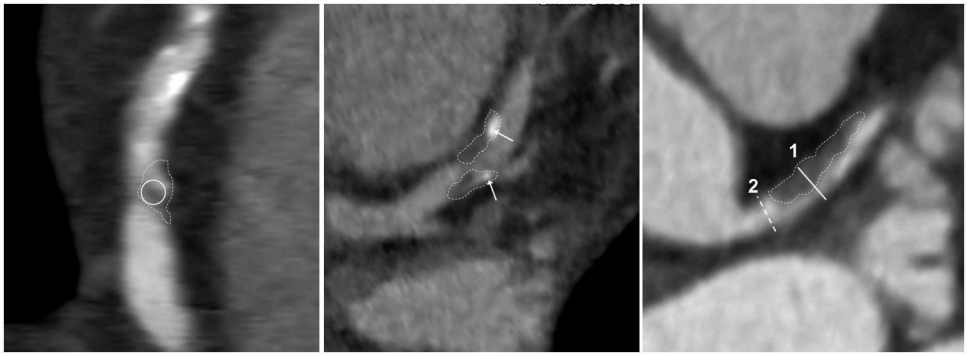

Figure 1.

Vulnerable plaque features evaluated in the study. The thin dotted lines trace out the plaques of interest in each panel. The non-calcified plaque in the left panel shows intra-plaque low-attenuation with <30 Hounsfield Units (inside the solid white circle), confirming presence of *low-attenuation plaque* (LAP). The middle panel shows *spotty calcification* (SC). The arrows denote high-intensity intra-plaque structures that occupy <90° of vessel circumference in short axis and measure <3mm in greatest dimension. *Positive remodeling* (PR) is shown in the right panel. Maximal outer vessel diameter along the non-calcified plaque (1, solid white line) exceeds proximal reference (2, dashed white line) by >5%.

NIH-PA Author Manuscript
NIH-PA Author Manuscript
NIH-PA Author Manuscript

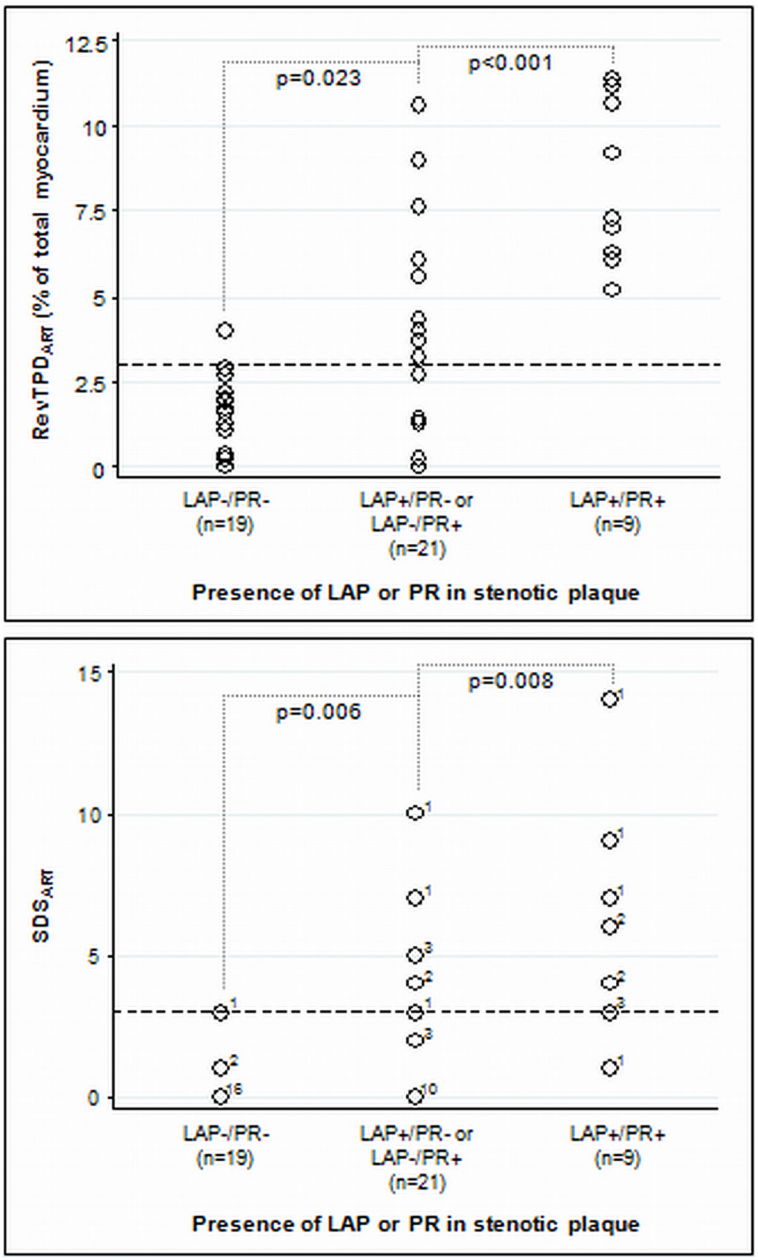

Figure 2.

Comparisons of reversible total perfusion defect and summed difference score corresponding to the diseased artery ($RevTPD_{ART}$ and SDS_{ART}, respectively) in study patients categorized by presence of low-attenuation plaque (LAP) and positive remodeling (PR) in the severely stenotic plaque. Both $RevTPD_{ART}$ and SDS_{ART} increased significantly from patients whose plaques exhibited neither LAP nor PR ($RevTPD_{ART}$ 1.3±1.2%,, SDS_{ART} 0.3±0.7) to patients whose plaques exhibited 1 of the 2 features ($RevTPD_{ART}$ 3.2±3.2%, SDS_{ART} 2.3±2.8) to patients whose plaques exhibited both features ($RevTPD_{ART}$ 8.3±2.4%, SDS_{ART} 6.0±3.8). In the bottom graph (SDS_{ART} results), the value immediately to the right of each circle indicates the number of patients with the finding (for example: 16 LAP−/PR− patients had SDS_{ART} of 0). The dotted lines represent the 3% $RevTPD_{ART}$ threshold and the 3 point SDS_{ART} threshold for significant myocardial hypoperfusion.

NIH-PA Author Manuscript
NIH-PA Author Manuscript
NIH-PA Author Manuscript

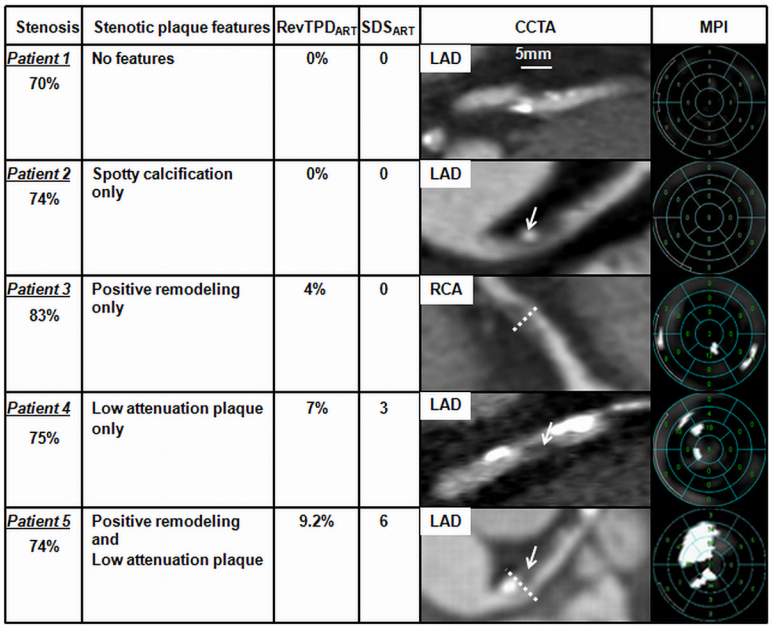

Figure 3.

Examples of severely stenotic plaques, presence of spotty calcification, positive remodeling and/or low attenuation plaque content, and corresponding regional myocardial hypoperfusion. Stenosis severity was quantified using coronary CT angiography (CCTA) as described in Methods.

Patient 1 has a severe proximal LAD stenosis from a plaque not exhibiting any of the features studied. There are 2 spotty calcifications distal to the plaque of interest; RevTPD$_{ART}$ was 0% and SDS$_{ART}$ was 0. ***Patient 2*** has a severe proximal LAD stenosis from a plaque exhibiting only spotty calcification (arrow); RevTPD$_{ART}$ was 0% and SDS$_{ART}$ was 0. ***Patient 3*** has a severe proximal RCA stenosis from a plaque exhibiting only positive remodeling (dotted line); RevTPD$_{ART}$ was 4% and SDS$_{ART}$ was 0. ***Patient 4*** has a severe proximal LAD stenosis from a plaque exhibiting only low attenuation plaque content (arrow, black area, Hounsfield unit <30); RevTPD$_{ART}$ was 7% and SDS$_{ART}$ was 3. ***Patient 5*** has a severe proximal LAD stenosis from a plaque exhibiting both positive remodeling (dotted line) and low attenuation plaque content (arrow); RevTPD$_{ART}$ was 9.2% and SDS$_{ART}$ was 6.

(LAD - left anterior descending coronary artery; MPI - myocardial perfusion imaging; RCA - right coronary artery; RevTPD$_{ART}$ - reversible total perfusion defect corresponding to the diseased artery; SDS$_{ART}$ - summed difference score corresponding to the diseased artery)

NIH-PA Author Manuscript NIH-PA Author Manuscript NIH-PA Author Manuscript

Table 1

Demographic characteristics of study patients and anatomic features of severely stenotic plaques evaluated (shown as median with inter-quartile range or as raw number and corresponding %)

		Categorization by $RevTPD_{ART}$			Categorization by PR and LAP		
	Total (n=49)	**≥3% (n=20)**	**<3% (n=29)**	**p-value***	**PR+ or LAP+ (n=30)**	**PR− and LAP− (n=19)**	**p-value†**
Demographic data							
Age (years)	66 (58,72)	66 (57,74)	66 (69,72)	0.855	66 (58,75)	62 (57,70)	0.334
Men	34 (69)	14 (70)	20 (69)	0.938	21 (70)	13 (68)	0.907
Diabetes	16 (33)	12 (60)	4 (14)	0.001	13 (43)	3 (16)	0.045
Hypertension	28 (57)	13 (65)	15 (52)	0.356	19 (63)	9 (48)	0.271
Dyslipidemia	41 (84)	17 (85)	24 (83)	0.835	25 (83)	16 (84)	0.935
Active smoking	11 (22)	6 (30)	5 (17)	0.293	7 (23)	4 (21)	0.852
Family CAD history	19 (39)	7 (35)	12 (41)	0.652	10 (33)	9 (47)	0.326
Reason for evaluation:				0.945			0.656
Chest pain or dyspnea	37 (75)	15 (75)	22 (76)	-	22 (73)	15 (79)	-
Other	12 (25)	5 (25)	7 (23)	-	8 (27)	4 (21)	-
PET-MPI	13 (27)	7 (35)	6 (21)	0.265	9 (30)	4 (21)	0.489
CCTA plaque data							
Diameter stenosis (%)	75 (71,85)	75 (73,85)	75 (71,86)	0.775	75 (73,83)	76 (73,82)	0.813
Artery affected				0.776			0.682
Left anterior descending	29 (59)	13 (65)	16 (55)	-	17 (57)	12 (63)	-
Left circumflex	8 (16)	3 (15)	5 (17)	-	6 (20)	2 (11)	-
Right coronary	12 (25)	4 (20)	8 (28)	-	7 (23)	5 (26)	-
In proximal segment	33 (67)	15 (75)	18 (62)	0.343	21 (70)	12 (63)	0.619
Stenosis ≥50% distal to plaque	7 (14)	2 (10)	5 (17)	0.476	5 (17)	2 (11)	0.550
Plaque length (mm)	9.4 (6,13)	9.2 (7,12)	9.4 (6,14)	0.895	9.7 (8,13)	8.9 (5,14)	0.356
LAP present (LAP+)	18 (37)	14 (70)	4 (14)	<0.001	18 (60)	-	-
PR present (PR+)	21 (43)	14 (70)	7 (24)	0.001	21 (70)	-	-
SC present	21 (43)	11 (55)	10 (34)	0.154	14 (47)	7 (37)	0.498
Contains LAP and PR	9 (18)	9 (45)	0 (0)	<0.001	9 (30)	-	-

NIH-PA Author Manuscript
NIH-PA Author Manuscript
NIH-PA Author Manuscript

[*] p-value compares patients with $RevTPD_{ART} \geq 3\%$ to patients with $RevTPD_{ART} < 3\%$.

[†] p-value compares patients with LAP or PR to patients without either feature.

CAD = coronary artery disease; CCTA = coronary computed tomographic angiography; LAP = low attenuation plaque; PET-MPI = positron-emission tomographic myocardial perfusion imaging; PR = positive remodeling; $RevTPD_{ART}$ = reversible total perfusion defect corresponding to the affected artery; SC = spotty calcification

NIH-PA Author Manuscript NIH-PA Author Manuscript NIH-PA Author Manuscript

Table 2

Results of multivariable linear regression analyses to assess relationships of LAP, PR, and SC to continuous measures of myocardial hypoperfusion.

	$RevTPD_{ART}$			SDS_{ART}		
	Beta	**95% CI**	**p-value**	**Beta**	**95% CI**	**p-value**
Presence of LAP	2.70	0.90 to 4.49	0.004	2.58	0.89 to 4.27	0.004
Presence of PR	2.88	1.30 to 4.47	0.001	2.08	0.59 to 3.56	0.007
Presence of SC	0.14	−1.52 to 1.80	0.863	0.14	−1.42 to 1.70	0.854
Diabetes	1.44	−0.35 to 3.23	0.111	0.87	−0.81 to 2.55	0.301
Smoking	1.04	−0.78 to 2.87	0.254	1.28	−0.43 to 3.00	0.138
Coronary artery distribution	0.46	−1.18 to 2.11	0.573	0.60	−0.94 to 2.15	0.435
Stenosis severity (per %)	5.70	−6.57 to 17.96	0.353	2.38	−9.14 to 13.90	0.679
Proximal location	−0.18	−1.91 to 1.55	0.835	−0.11	−1.73 to 1.51	0.892
Whether PET was performed	0.90	−1.12 to 2.91	0.375	2.06	0.17 to 3.95	0.034

CI = confidence interval; LAP = low attenuation plaque; PR = positive remodeling, $RevTPD_{ART}$ = reversible total perfusion defect corresponding to diseased artery, SDS_{ART} = summed difference score corresponding to the affected artery

NIH-PA Author Manuscript
NIH-PA Author Manuscript
NIH-PA Author Manuscript

Table 3

Results of multivariable logistic regression analyses to assess relationships of LAP, PR, and SC to binary measures of significant myocardial hypoperfusion.

	$RevTPD_{ART}$≥3%			SDS_{ART}≥3		
	OR	**95%CI**	**p-value**	**OR**	**95%CI**	**p-value**
Presence of LAP	69.4	2.6 to 1883.0	0.012	15.3	1.5 to 160.3	0.023
Presence of PR	27.4	2.0 to 371.6	0.013	27.4	1.25 to 600.8	0.036
Presence of SC	2.0	0.2 to 21.1	0.581	5.4	0.5 to 54.3	0.154
Diabetes	25.4	1.3 to 481.3	0.031	6.0	0.3 to 109.8	0.226
Smoking	18.3	0.9 to 383.8	0.061	17.8	1.2 to 256.8	0.035
Coronary artery distribution	1.0	0.1 to 10.2	0.982	1.3	0.2 to 10.1	0.776
Stenosis severity (per %)	1.5	0.0 to >10000	0.971	0.0	0.0 to >10000	0.436
Proximal location	0.8	0.1 to 9.0	0.851	0.6	0.1 to 5.9	0.665
Whether PET was performed	1.9	0.1 to 29.0	0.657	9.2	0.5 to 166.2	0.133

CI = confidence interval; LAP = low attenuation plaque; OR = odds ratio; PR = positive remodeling, $RevTPD_{ART}$ = reversible total perfusion defect corresponding to diseased artery, SDS_{ART} = summed difference score corresponding to the affected artery